Joints with dowel-type fasteners - Theory

STEP lecture C3
B.O. Hilson
University of Brighton

Objectives

To define embedding strength and to demonstrate how it is measured. To develop the ultimate load equations for laterally loaded joints with dowel-type fasteners and to show how they may be represented graphically.

Prerequisite

C1 Mechanical timber joints - General

Summary

Embedding strength is defined and the parameters to be controlled in the design of embedment test apparatus are described. Johansen's equations for the ultimate strength of timber-to-timber joints, and steel-to-timber joints, are developed. Graphical representations of the timber-to-timber equations based on Möller are shown.

Introduction

Laterally loaded joints with dowel-type fasteners are illustrated in Figure 1. Typical dowels that might be used include nails, staples, screws and bolts.

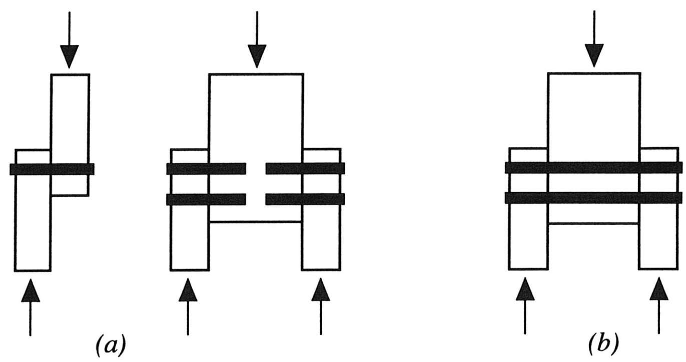

Figure 1 *Laterally loaded joints with dowel-type fasteners. (a) Dowels in single shear (i.e. one shear plane per dowel), (b) Dowels in double shear (i.e. two shear planes per dowel).*

In the past the working load design values for these types of joint have been determined from the results of short-duration tests on relatively small numbers of replicate joints. One approach made estimates of lower percentile values, eg lower first percentile, assuming a normal distribution, and these were then divided by a factor to account for safety and workmanship and to reduce the strength to an equivalent long-duration load value.

The data available from the above tests are generally insufficient to enable reliable estimates to be made of the characteristic strengths required for EC5. To obtain the data by mass testing would have been prohibitive because of the many combinations that are possible in practice. Consequently, techniques have been developed which enable characteristic values to be predicted from material properties and joint geometry.

The equations used in EC5: Part 1-1 are based upon a theory first developed by Johansen (1949). The equations predict the ultimate strength of a dowel-type joint due to either a bearing failure of the joint members or the simultaneous development of a bearing failure of the joint members and plastic hinge formation in the fastener. The precise mode of failure is determined by the joint geometry and the material properties namely the fastener yield moment and the embedding strengths of the timber or wood-based materials.

Many researchers have carried out tests to validate Johansen's equations including Möller (1951), Aune and Patton-Mallory (1986), Hilson et al. (1990) and in every case, provided the effects of friction between members and axial force development have been minimised, good agreement has been found between experiment and theory.

Material properties

The embedding strength of timber, or of a wood-based material, is defined as the ultimate stress obtained from a special type of joint test called an embedment test. A typical test arrangement is illustrated in Figure 2.

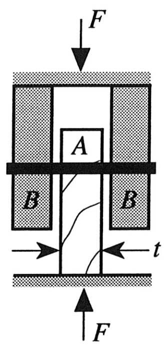

Figure 2 *Typical embedment test arrangement. A - specimen, B - steel side plates rigidly clamping fastener.*

Bending deformation of the dowel must be minimised and this can be achieved by clamping the ends of the dowel in the steel side plates and by limiting the thickness of the test specimen - typically to twice the dowel diameter.

A typical load-embedment characteristic is shown in Figure 3 and the embedding strength is defined as the maximum load, or the load at a specified limiting deformation, divided by the projected area of the dowel in the specimen i.e

$$f_h = \frac{F_{max}}{dt} \qquad (1)$$

where t is the thickness of the test specimen and d is the dowel diameter.

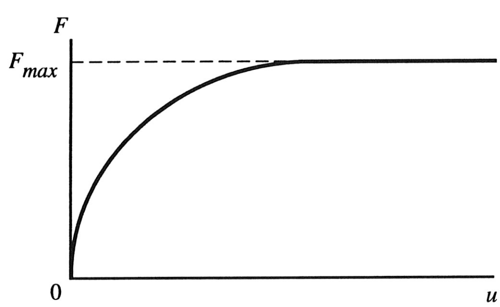

Figure 3 *Typical load-embedment characteristic.*

The embedment, u, is the movement of the dowel relative to the specimen, i.e. of BB relative to A in Figure 2.

Further guidance on the determination of embedding strength is given in EN 383 "Determination of embedding strength and foundation values for dowel type fasteners" and suitable apparatuses for measuring embedding strength are described by Rodd et al. (1987).

Even in the most carefully designed apparatus some slight movements, in addition to the embedment of the dowel in the specimen, will occur. The characteristics of the apparatus should be measured, therefore, by carrying out a test with a rigid, (e.g. steel), central member and a tightly fitting dowel of the same diameter and surface condition as those under investigation. This characteristic should then be deducted from the normal test characteristics to obtain the true load-embedment characteristics.

Procedures for measuring the yield moment of nails are set out in EN 409 "Determination of the yield moment for dowel-type fasteners - nails".

EC5: Part 1-1: 6.2

Johansen's equations. Fasteners in single shear

In deriving Johansens's ultimate load equations it is assumed that both the fastener and the timber are ideal rigid-plastic materials, e.g. the load-embedment characteristic for the timber is as shown in Figure 4. This approximation simplifies the analysis and makes little difference to the final result.

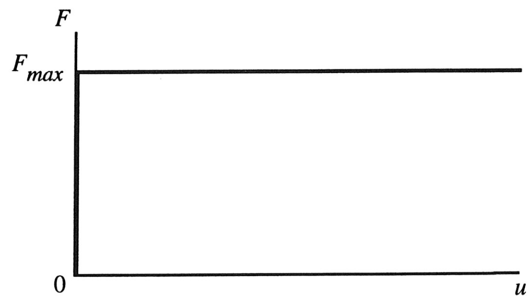

Figure 4 Simplified load-embedment characteristic.

The following notation is used:

t_1 and t_2 are the timber thicknesses or fastener penetrations,
$f_{h,1,k}$ is the characteristic embedding strength corresponding to t_1.
$f_{h,2,k}$ is the characteristic embedding strength corresponding to t_2,
$\beta = \frac{f_{h,2,d}}{f_{h,1,d}}$ where $f_{h,d} = \frac{k_{mod} f_{h,k}}{\gamma_M}$ is the design value of embedding strength,
d is the diameter of fastener,
$M_{y,k}$ is the characteristic yield moment for fastener,
$M_{y,d} = \frac{M_{y,k}}{\gamma_M}$ is the design value of fastener yield moment and
R_d is the design resistance per shear plane.

The numbering of the failure modes used in the following derivations follows that used by Johansen.

Failure mode 1b

From Figure 5 $R_d = f_{h,1,d}\, t_1\, d$ (2)

From Figure 6 $R_d = f_{h,2,d}\, t_2\, d$

$R_d = \beta\, f_{h,1,d}\, t_2\, d$ (3)

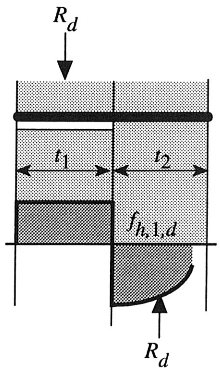

Figure 5 Mode 1b failure in t_1.

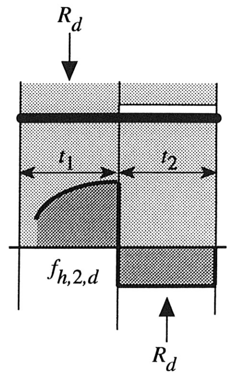

Figure 6 Mode 1b failure in t_2.

Failure mode 1a

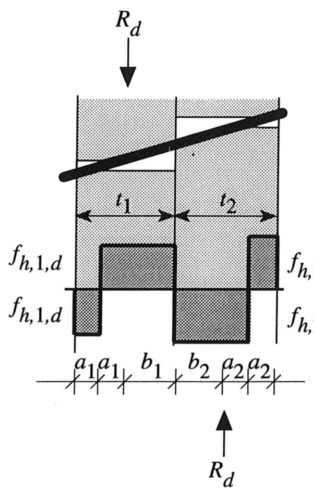

Figure 7 Mode 1a failure.

$$R_d = f_{h,1,d}\, d\, b_1 = f_{h,2,d}\, d\, b_2 = \beta\, f_{h,1,d}\, d\, b_2$$

$$b_1 = \beta\, b_2$$

Moment at interface $= f_{h,1,d}\, d \left(\frac{b_1^2}{2} - a_1^2 \right)$

$$= f_{h,2,d}\, d \left(a_2^2 - \frac{b_2^2}{2} \right)$$

$$= \beta\, f_{h,1,d}\, d \left(a_2^2 - \frac{b_2^2}{2} \right)$$

Equating and putting $b_2 = \dfrac{b_1}{\beta}$ **gives :**

$$\frac{b_1^2}{2}\,\frac{\beta+1}{\beta} = \beta a_2^2 + a_1^2$$

$$a_1 = \frac{t_1 - b_1}{2} \text{ and } a_2 = \frac{t_2 - b_2}{2} = \frac{\beta\, t_2 - b_1}{2\beta}$$

Substitution gives:

$$b_1^2\left(\frac{1+\beta}{\beta}\right) + 2\,b_1\,(t_1 + t_2) - (t_1^2 + \beta\, t_2^2) = 0$$

Solving for b_1 gives:

$$b_1 = \frac{t_1}{1+\beta}\left[\sqrt{\beta + 2\,\beta^2\left[1 + \frac{t_2}{t_1} + \left(\frac{t_2}{t_1}\right)^2\right] + \beta^3\left(\frac{t_2}{t_1}\right)^2} - \beta\left(1 + \frac{t_2}{t_1}\right)\right]$$

$$R_d = f_{h,l,d}\, d\, b_1$$

$$R_d = \frac{f_{h,l,d}\, d\, t_1}{1+\beta}\left[\sqrt{\beta + 2\,\beta^2\left[1 + \frac{t_2}{t_1} + \left(\frac{t_2}{t_1}\right)^2\right] + \beta^3\left(\frac{t_2}{t_1}\right)^2} - \beta\left(1 + \frac{t_2}{t_1}\right)\right] \qquad (4)$$

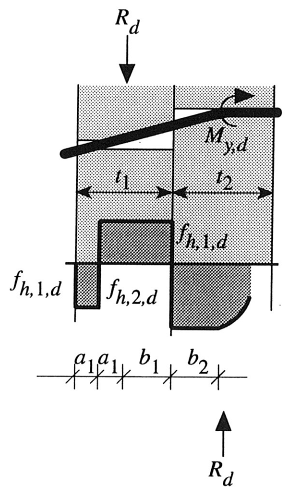

Figure 8 Mode 2a failure.

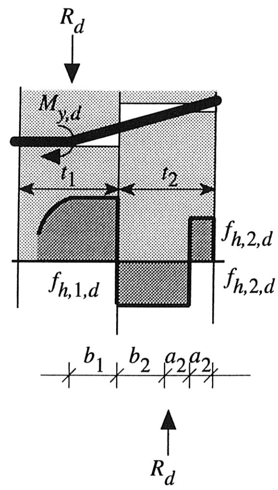

Figure 9 Mode 2b failure.

Failure mode 2a (from Figure 8)

At M_{max} shear $= 0$

$$f_{h,1,d}\; d\; b_1 = f_{h,2,d}\; d\; b_2 = \beta\, f_{h,1,d}\; d\; b_2$$

$$b_1 = \beta\; b_2$$

$$M_{y,d} = -f_{h,2,d}\,d\,\frac{b_2^2}{2} + f_{h,1,d}\,d\,(b_1 + a_1)\left(b_2 + \frac{b_1 + a_1}{2}\right) - f_{h,1,d}\,d\,a_1\left(b_1 + b_2 + \frac{3\,a_1}{2}\right)$$

Substituting $f_{h,2,d} = \beta f_{h,1,d}$ **and** $a_1 = \frac{t_1 - b_1}{2}$ **gives :**

$$b_1^2 + t_1\,\frac{2\beta}{2+\beta}\,b_1 - \frac{\beta\,t_1^2}{2+\beta} - \frac{M_{y,d}}{f_{h,1,d}\,d}\,\frac{4\beta}{2+\beta} = 0$$

then $b_1 = \frac{t_1}{2+\beta}\left[\sqrt{2\beta(1+\beta) + \frac{4\beta(2+\beta)M_{y,d}}{f_{h,1,d}\,d\,t_1^2}} - \beta\right]$

and $R_d = f_{h,1,d}\;d\;b_1$

$$R_d = \frac{f_{h,1,d}\,d\,t_1}{2+\beta}\left[\sqrt{2\beta(1+\beta) + \frac{4\beta(2+\beta)M_{y,d}}{f_{h,1,d}\,d\,t_1^2}} - \beta\right] \qquad (5)$$

Failure mode 2b (from Figure 9)

As before $b_1 = \beta\;b_2$

$$M_{y,d} = f_{h,1,d}\,d\left[\frac{-b_1^2}{2} + \beta\,b_2\left(b_1 + \frac{b_2}{2}\right) + \beta\,a_2\left(b_1 + t_2 - \frac{3\,a_2}{2}\right) - \beta\,a_2\left(b_1 + t_2 - \frac{a_2}{2}\right)\right]$$

Substituting $b_1 = \beta\,b_2$ **and** $a_2 = \frac{t_2 - b_2}{2}$ **gives :**

$$b_2^2 + \frac{\beta}{2}\,\frac{4\,t_2\,b_2}{\beta(2\beta+1)} - \left(\frac{\beta\,t_2^2}{4} + \frac{M_{y,d}}{f_{h,1,d}\,d}\right)\frac{4}{\beta(2\beta+1)} = 0$$

$$b_2 = \frac{-t_2}{2\beta+1} + \sqrt{\frac{t_2^2}{(2\beta+1)^2} + \frac{t_2^2}{2\beta+1} + \frac{4M_{y,d}}{f_{h,1,d}\,d\,\beta(2\beta+1)}}$$

$$R_d = \beta f_{h,1,d}\,d\,b_2$$

$$R_d = \frac{f_{h,1,d}\;d\;t_2}{1+2\beta}\left[\sqrt{2\beta^2(1+\beta) + \frac{4\beta(1+2\beta)M_{y,d}}{f_{h,1,d}\;d\;t_2^2}} - \beta\right] \qquad (6)$$

Failure Mode 3 (from Figure 10)

$$M_{y,d} + M_{y,d} = f_{h,1,d}\;d\;b_1\left(b_2 + \frac{b_1}{2}\right) - \beta\;f_{h,1,d}\;d\;\frac{b_2^2}{2}$$

$$b_2 = \frac{b_1}{\beta}$$

$$b_1 = \sqrt{\frac{2M_{y,d}}{f_{h,1,d}\, d}} \sqrt{\frac{2\beta}{1+\beta}}$$

$$R_d = f_{h,1,d}\, d\, b_1 = \sqrt{\frac{2\beta}{1+\beta}} \sqrt{2M_{y,d}\, f_{h,1,d}\, d} \qquad (7)$$

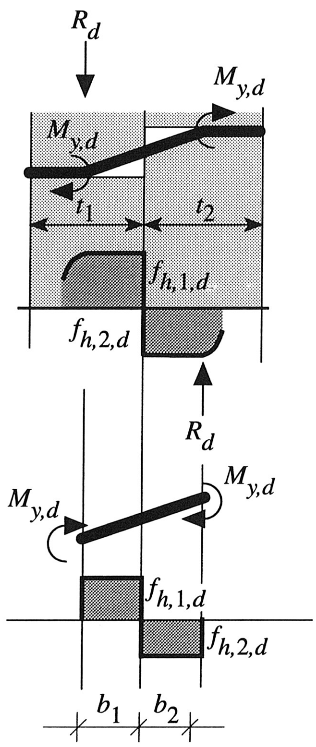

Figure 10 Mode 3 failure.

Johansen's equations may also be derived using the Virtual Work approach (Aune and Patton-Mallory, 1986).

Additional resistance

As the fastener deforms under load axial forces can develop for failure modes 2 and 3. These are caused by friction between the fastener and the timber and also by the constraints produced by the heads of nails and the washer assemblies in bolts.

The force in the inclined part of the fastener will have a component parallel to the applied load and will, therefore, enhance the resistance. EC5 takes this effect into account by enhancing the resistance for modes 2 and 3 failures by 10 per cent.

In an actual joint the load carrying capacity will correspond to the lowest value obtained for R_d by substituting into the full set of equations. The equation giving the lowest capacity will also identify the failure mode.

Möller charts

Möller (1951) represented the Johansen equations for single shear, in cases for which $\beta = 1$, by a graphical representation. In this lecture the Möller chart has been modified to incorporate the 10% enhancement for modes 2 and 3 failures and is shown in Figure 11. It should be noted that in this chart t_2 is the larger thickness or embedded length. Similar charts may be produced for other values of β. By calculating the two dimensionless parameters $\frac{t_2}{t_1}$ and $\frac{t_1}{\sqrt{\frac{M_{y,d}}{f_{h,d}d}}}$ a point may be found on the chart, the appropriate failure mode identified and hence the appropriate equation chosen.

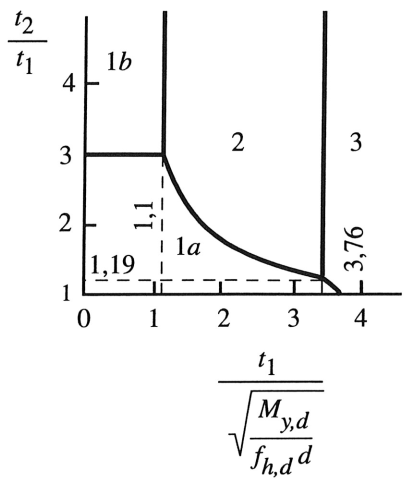

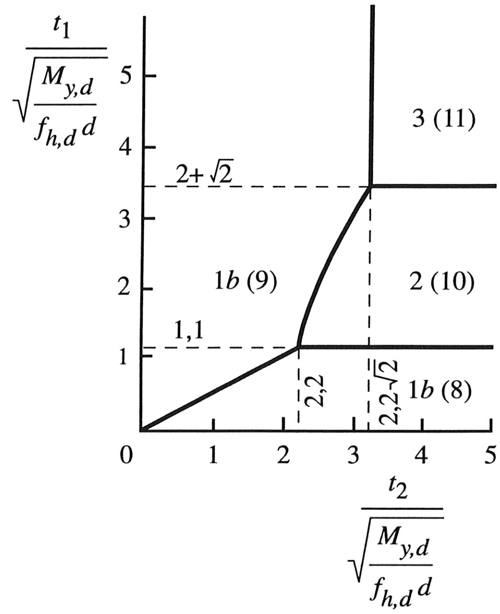

Figure 11 Modified Möller chart - single shear (β = 1).

Figure 12 Modified Möller chart - double shear (β = 1).

Johansens's equations. Fasteners in double shear

Using the same basic approach, Johansen equations for fasteners in double shear may be developed. The resulting equations are as follows:

$R_d = f_{h,1,d}\, t_1\, d$ Mode 1b (Figure 5) (8)

$R_d = 0{,}5\, f_{h,1,d}\, t_2\, d\, \beta$ Mode 1b (Figure 6) (9)

$$R_d = \frac{f_{h,1,d} t_1 d}{2+\beta}\left[\sqrt{2\beta(1+\beta) + \frac{4\beta(2+\beta)M_{y,d}}{f_{h,1,d} d t_1^2}} - \beta\right]$$ Mode 2 (Figure 8 or 9) (10)

$$R_d = \sqrt{\frac{2\beta}{1+\beta}}\sqrt{2\, M_{y,d} f_{h,1,d}\, d}$$ Mode 3 (Figure 10) (11)

The Figure number refers to the diagram showing half of the corresponding symmetrical double shear joint.

In these equations t_2 is the central member thickness and t_1 the thickness of an outer timber or the penetration in an outer timber whichever is the smaller. In each case R_d represents the resistance of one shear plane so the resistance of the whole joint is normally $2R_d$. The equations apply to symmetrical double shear joints - other geometries may be analysed using the same principles.

Again to allow for axial force effects the modes 2 and 3 values may be enhanced by 10%. A modified Möller chart incorporating the enhancement is shown in Figure 12.

Johansen's equations for steel-to-timber joints

In steel-to-timber joints, provided the steel plate is thick enough, then for modes 2 and 3 failures the plastic hinges will move to the interface between the steel and the timber and different Johansen equations may be developed. A steel plate thickness at least equal to the fastener diameter is normally assumed sufficient for this approach to apply. Using the above assumption, the following equations may be derived:

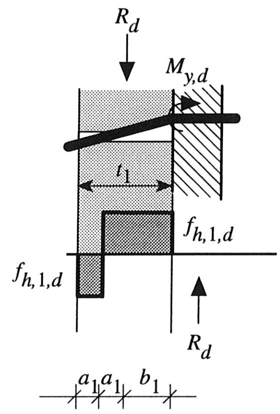

Figure 13 Mode 2 failure - thick steel plate.

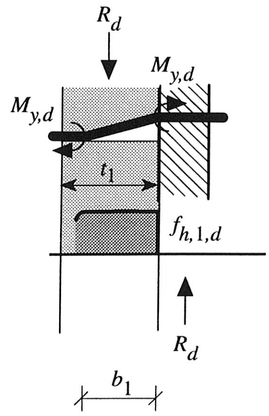

Figure 14 Mode 3 Failure - thick steel plate.

Thick steel plates - Mode 2

From Figure 13

$$M_{y,d} = f_{h,1,d}\, d\, \frac{b_1^2}{2} + f_{h,1,d}\, d\, a_1 \left(t_1 - \frac{3a_1}{2}\right) - f_{h,1,d}\, d\, a_1 \left(t_1 - \frac{a_1}{2}\right)$$

substituting $a_1 = \dfrac{t_1 - b_1}{2}$ **gives :**

$$b_1^2 + 2\, t_1\, b_1 - \left(t_1^2 + \frac{4M_{y,d}}{f_{h,1,d}\, d}\right) = 0$$

$$b_1 = t_1 \left[\sqrt{2 + \frac{4M_{y,d}}{f_{h,1,d}\, d\, t_1^2}} - 1\right]$$

$$R_d = f_{h,1,d}\, d\, b_1 = f_{h,1,d}\, d\, t_1 \left[\sqrt{2 + \frac{4M_{y,d}}{f_{h,1,d}\, d\, t_1^2}} - 1\right] \qquad (12)$$

Thick steel plates - Mode 3

From Figure 14

$$2M_{y,d} = f_{h,1,d}\, d \frac{b_1^2}{2}$$

$$b_1 = 2\sqrt{\frac{M_{y,d}}{f_{h,1,d}\, d}}$$

$$R_d = f_{h,1,d}\, d\, b_1 = 2\sqrt{M_{y,d}\, f_{h,1,d}\, d}$$

$$R_d = 1{,}4\sqrt{2M_{y,d}\, f_{h,1,d}\, d} \qquad (13)$$

Thick steel plates - Mode 1b

$R_d = f_{h,1,d}\ t_1\ d$ as before (14)

Again for modes 2 and 3 a 10% increase is suggested in EC5 to allow for axial force effects.

Thin steel plates
For thin steel plates the plate will be unable to provide the rotational resistance to develop a plastic hinge in the fastener and so the EC5 equations have been developed assuming no moment of resistance at the interface.

EC5 defines a thin steel plate as one having a thickness equal to, or less than, half the dowel diameter.

Using the above assumption the following equations may be derived:

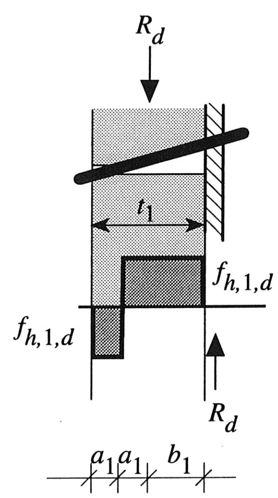

Figure 15 Mode 1a failure - thin steel plate.

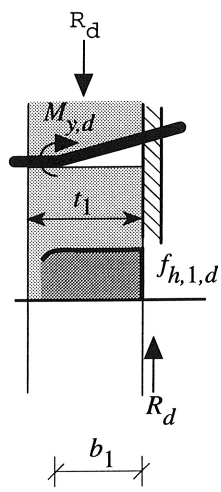

Figure 16 Mode 2 failure - thin steel plate.

Thin steel plates - Mode 1a
From Figure 15 moment at interface = 0

$$0 = f_{h,1,d}\, d \left(\frac{b_1^2}{2} - a_1^2 \right)$$

$$a_1 = \frac{t_1 - b_1}{2} \quad \text{and} \quad b_1^2 + 2\, t_1\, b_1 - t_1^2 = 0$$

$$b_1 = t_1 (\sqrt{2} - 1)$$

$$R_d = f_{h,1,d}\, d\, b_1 = 0{,}4\, f_{h,1,d}\, d\, t_1 \qquad (15)$$

Thin steel plates - Mode 2
From Figure 16 moment at interface = 0

$$0 = -M_{y,d} + f_{h,1,d}\, d\, \frac{b_1^2}{2} \quad \text{and} \quad b_1 = \sqrt{\frac{2\, M_{y,d}}{f_{h,1,d}\, d}}$$

$$R_d = f_{h,1,d}\, d\, b_1 = \sqrt{2\, M_{y,d}\, f_{h,1,d}\, d}$$

Allowing 10% increase for axial force effects gives

$$R_d = 1{,}1 \sqrt{2\, M_{y,d}\, f_{h,1,d}\, d} \qquad (16)$$

Note: Double shear joint - Centre member of thin steel
The same equations apply as for thick steel plates since the symmetry of the joint enables a plastic hinge to form in the steel plate, provided the plate is strong enough to resist the applied forces.

For steel plate thicknesses between 0,5*d* and *d* EC5 suggests that resistances should be determined by linear interpolation between thick and thin plate values.

References

Aune, P. and Patton-Mallory, M. (1986). Lateral load-bearing capacity of nailed joints based on the yield theory - Theoretical development and experimental verification. US Department of Agriculture, Forest Products Laboratory, Research Papers FPL 469 & 470.

Hilson, B.O., Whale, L.R.J. and Smith, I. (1990). Characteristic properties of nailed and bolted joints under short-term lateral load. Part 5 - Appraisal of current design data in BS5268:Part 2:1984 Structural Use of Timber. J. Inst. Wood Sci. 11(6) 208-212.

Johansen, K.W. (1949). Theory of timber connections. International Association of Bridge and Structural Engineering. Publication No. 9:249-262. Bern

Möller, T. (1951). En ny metod för beräkning av spikförband. Report No 117, Chalmers University of Technology, Sweden

Rodd, P.D., Anderson, C., Whale, L.R.J. and Smith, I. (1987). Characteristic properties of nailed and bolted joints under short term lateral load. Part 2 - Embedment test apparatus for wood and wood-based sheet materials. J. Inst. Wood Sci. 11(2): 60-64.